

Reconstruction of spatial structure of ionospheric perturbation from data measured at a dense GPS network (GEONET)

E.L. Afraimovich, V.V. Kiryushkin, N.P. Perevalova, and M.V. Mas'kin

*Institute of Solar-Terrestrial Physics,
Siberian Branch of the Russian Academy of Sciences, Irkutsk*

Received August 18, 2006

We present a method of reconstruction of spatiotemporal structure of ionospheric perturbations, based on construction of instant pattern of distribution of increments of the total electron content (TEC) in the ionosphere, obtained from data measured at the GPS Earth Observation Network (GEONET), which consists of more than 1000 double-frequency GPS receivers located throughout the territory of Japan. Reconstruction of spatial structure of perturbations is performed by constructing a set of TEC increments at ionospheric points for a given moment in time and through approximation of this set with the help of splines on a uniform and stationary grid. This method was tested in reconstructing spatial structure of perturbations, specially modeled for conditions of powerful earthquake near Hokkaido Island on September 25, 2003. The test results showed that this method is capable of reconstructing spatiotemporal structure of ionospheric perturbations and track the dynamics of their variations with high time resolution.

Introduction

In recent years, different technologies of using the Global Positioning System (GPS) have actively been developed for remote monitoring of the ionosphere. Development of widespread networks of GPS receivers has led to the fact that presently the Earth's ionosphere is scrutinized simultaneously by thousands and tens of thousands of receiver-satellite paths. The possibility of using the large number of sounding paths permits solving the problems of reconstruction of spatial structure and time dynamics of ionospheric perturbations of different classes.

Based on data measured with GPS receivers of world geodynamic network IGS, the technology of global mapping (GIMs) the total electron content (TEC) of the ionosphere has been developed.¹ The GIM spatial (5° in longitude and 2.5° in latitude) and time (15–120 min) resolution makes it possible to study large-scale ionospheric processes under quiet and perturbed conditions.

Reconstruction of medium- and small-scale ionospheric perturbations requires denser network of receivers to ensure necessary accuracy of interpolation of TEC measurement data. Presently, this information potential is shared by regional networks of GPS receivers in North America, Europe, and Japan. In Japan, the regional GEONET network (<http://mekira.gsi.go.jp>; <http://terras.gsi.go.jp>) unites about 1000 ground-based double-frequency GPS receivers (number of receiver-satellite paths reaches 4000 to 6000).

Using GEONET data, Saito et al.² plotted two-dimensional maps of TEC perturbations over Japan.

The maps have spatial resolution 0.15° in latitude and longitude and 30-s time resolution. The maps were generated by averaging the measurement data of TEC increments obtained for receiver-satellite paths within a chosen spatial cell.

Most promising method for reconstruction of spatial structure of ionospheric perturbations is, in our opinion, the interpolation of individual TEC readouts using spline functions.^{3,4} The spline interpolation does not limit the spatial resolution of reconstructed pattern by initially chosen cell size. We present a method of reconstruction of spatial structure of ionospheric perturbation through interpolation of TEC readouts obtained at a dense network of GPS receivers using spline surfaces.

Initial data

For validation of the method, the initial data were synthesized taking into account actual location of the GPS stations of GEONET network and real trajectories of GPS satellites in time interval 19:00–21:18 UT, embracing the time of the main earthquake shock near Hokkaido Island at 19:50 UT on September 25, 2003. The coordinates of 429 receiving stations belonging to the GEONET network are provided by Prof. K. Heki from Hokkaido University. The positions of these stations are indicated by triangles in Fig. 1.

Locations of the GPS satellites were determined from real measurement data from the receiving TSKB station (indicated by cross in Fig. 1). The TSKB station belongs to international geodesic network IGS, and its measurement data, together with measurement

data from other sites belonging to IGS network, are accessible in standard Receiver Independent Exchange (RINEX) format at <http://sopac.ucsd.edu/cgi-bin/dbDataByDate.cgi>.

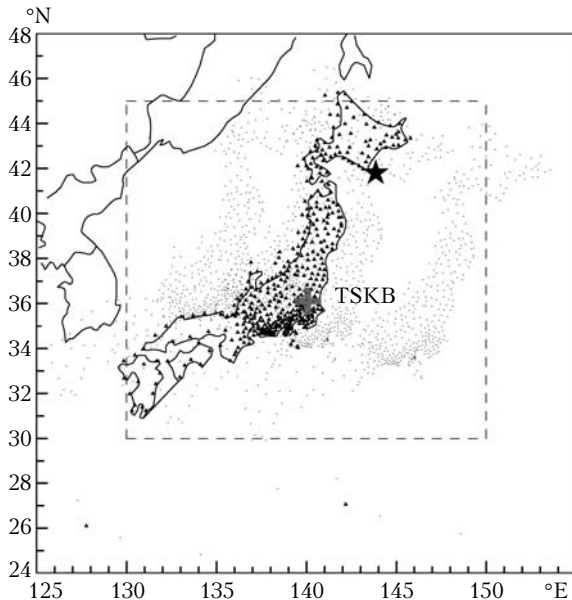


Fig. 1. Locations of the receiving GPS stations of GEONET network.

Data of RINEX files from TSKB station were converted into time series of azimuths and elevation angles of the paths formed by TSKB receiver and satellites with numbers PRN04, PRN10, PRN24, and PRN27, which were located in the zone of its radio visibility within the time interval 19:00–21:18 UT. Since all stations of GEONET network are located in a narrow latitude-longitude interval, the angular characteristics of receiver–satellite viewing paths can be considered to change insignificantly within this region. Therefore, the rays formed by the TSKB station and PRN04, PRN10, PRN24, and PRN27 satellites were translated in parallel direction to locations of each of the 429 receiving GPS stations of GEONET network. Owing to these transformations in the region, we obtained a dense GPS grid composed of $P = 1716$ receiver–satellite paths.

Modeling the TEC measurements

The TEC measurements along each of P synthesized paths of the GPS grid were modeled using the model of TEC measurements developed at Institute of Solar and Terrestrial Physics SB RAS.⁵

The model TEC value $I_{j,k}$ along j th receiver–satellite path for the k th moment in time is determined from the formula:

$$I_{j,k} = \int_0^D N(t_k, r, \alpha_{j,k}, \theta_{j,k}) dr, \quad (1)$$

where D is the slant range along the receiver–satellite path, $N(t_k, r, \alpha_{j,k}, \theta_{j,k})$ is the local electron concentration,

r is the position vector of the point on the receiver–satellite path, $\alpha_{j,k}$ and $\theta_{j,k}$ are, respectively, the azimuth and elevation angle of the j th receiver–satellite path at the k th moment in time.

The model of electron concentration $N(t_k, r, \alpha_{j,k}, \theta_{j,k})$ takes into account the altitude distribution of ionization and diurnal and latitude-longitude variations, which are determined by solar zenith angle, as well as irregular perturbations with lower amplitude and smaller spatial scale.

The irregular component of ionization was specified in the geocentric coordinate system in the form of spherical wave of ionospheric perturbation with the wave source at the point with coordinates Φ_e (latitude), Λ_e (longitude), and h_e (height above the Earth's surface):

$$N_d(t, R) = W_d(t, R) A_w \times \cos[\Omega_w(t - t_e) - K_w(R - R_e) + \varphi_0], \quad (2)$$

where R is the position vector of the current point on the path, $R_e = R_E + h_e$ is the position vector of source of perturbation, R_E is the Earth's radius, A_w is the amplitude, $\Omega_w = 2\pi/T_w$ is the frequency, $K_w = 2\pi/(T_w V_w)$ is the wave number, T_w is the period, V_w is the phase velocity of a spherical wave of perturbation, φ_0 is the initial phase of perturbation, $W_d(t, R)$ is the modulating envelope allowing one to obtain the perturbation of a “wave packet” type.

The TEC measurements were modeled for ionospheric conditions during strong earthquake near Hokkaido Island on September 25, 2003. Epicenter of the earthquake is denoted by a star in Fig. 1 (<http://www.neic.cr.usgs.gov>). The level of geomagnetic perturbation during the earthquake was found to be quite moderate ($D_{st} = 0-21$ nT, $K_p = 1-4$, <http://www.wdc.rl.ac.uk/cgi-bin/wdccl/secure/wdcdata>). In this regard, in modeling we specified parameters of regular ionization component, characteristic of the quiet midlatitude ionosphere.

The source of model spherical wave of perturbation was placed at the earthquake epicenter with $\Phi_e = 41.8^\circ\text{N}$, $\Lambda_e = 143.85^\circ\text{E}$ at the height of ionization maximum of ionosphere of $h_e = 350$ km. This corresponds to ideas that ionospheric perturbations from secondary source located above the epicenter at heights 200–300 km are generated during an earthquake,^{5,6} and it is consistent with the results of earlier studies on localization of the source of ionospheric perturbation caused by the earthquake near Hokkaido Island.⁷

Switch-on time of the source of spherical perturbation corresponds to the time of the main earthquake shock at $t_e = 19:50$ UT, while the parameters of the perturbation itself are characteristic for ionospheric wave inhomogeneities caused by the passage of shock acoustic wave generated during piston-like movements of the Earth's crust^{5,7}: $A_w = 15\%$, $V_w = 1000$ m/s, $T_w = 10$ min, and $\varphi_0 = 0$.

Figures 2a–d present examples of time variations of model values of “slant” (i.e., measured along slant path) TEC $I_j(t_k)$ for four receiver–satellite paths. The

generally accepted TEC unit is TECU (Total Electron Content Unit) which equals 10^{16} m^{-2} . It can be seen that, against the background of slow TEC variations (trend), there are high-frequency variations caused by passage of ionospheric perturbation wave.

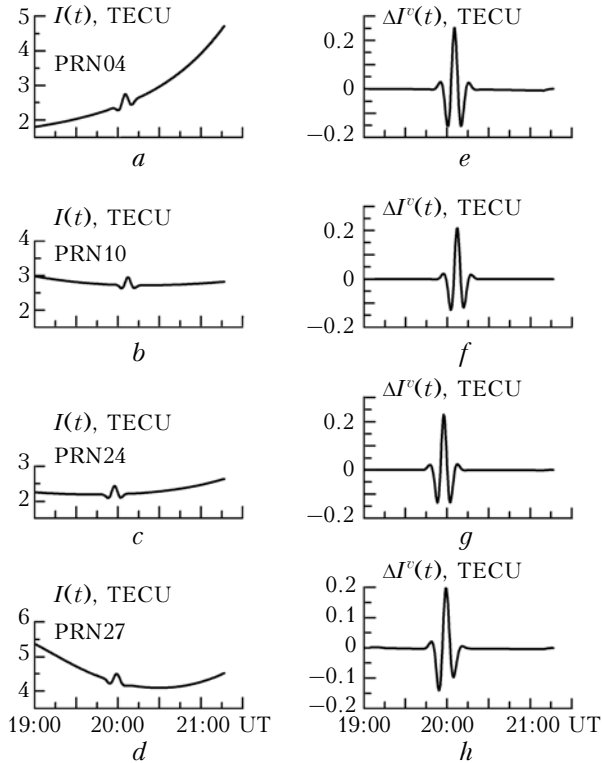


Fig. 2. Time variations of model values of “slant” TEC (a–d) and increments of “vertical” TEC (e–h).

Method of reconstruction of spatial structure of the ionospheric perturbation

It is assumed that TEC value obtained on receiver–satellite path corresponds to ionospheric point, namely the point of intersection of the path with the plane at the height of the ionization maximum. Geocentric coordinates $(\Phi_{j,k}, \Lambda_{j,k})$ of the ionospheric point are calculated based on the known coordinates of the receiving GPS stations, azimuths, and elevation angle of the path.⁵

“Slant” TEC values $I_j(t_k)$ were transformed to equivalent “vertical” ones $I_j^v(t_k)$.⁵ To separate out TEC increments caused by propagation of perturbation wave, we filtered the obtained time series of “vertical” TEC by removing the trend with 10-min time window corresponding to the period of model spherical wave. After such a filtering, we obtained time series $\Delta I_j^v(t_k)$ of increments of “vertical” TEC at the corresponding ionospheric points $(\Phi_{j,k}, \Lambda_{j,k})$. The increments of “vertical” TEC $\Delta I_j^v(t_k)$ for four receiver–satellite paths are plotted in Figs. 2e–h.

The instantaneous pattern of TEC perturbation at $t_k = t_x$ was plotted by sampling from all obtained

series of $\Delta I_{j,x}^v$ and $(\Phi_{j,k}, \Lambda_{j,k})$ values ($j = 1, \dots, P$). The spatial distribution of ionospheric points at the time $t_x = 20:00$ UT is indicated in Fig. 1 by dots. Region totally covered with spatial readouts of TEC increments lies in the region $30\text{--}45^\circ$ in latitude and $130\text{--}150^\circ$ in longitude (shown by dashed lines in Fig. 1). Precisely in this region the spatial structure of ionospheric perturbation was reconstructed.

However, the ionospheric points are distributed nonuniformly in this region because the receiving GPS stations are spaced irregularly. In addition, the angular characteristics of the receiver–satellite paths change with time due to orbiting of the GPS satellites, also causing change of coordinates of the ionospheric points. Thus, readouts of TEC increments are obtained on nonuniform and non-stationary measurement grid. For interpolation of the obtained readouts, we used spline surface, representing spatial analog of the one-dimensional spline.^{3,4}

In context of the problem on reconstructing the spatial function of distribution of TEC increments $\Delta I(\Phi, \Lambda)$ over the latitude–longitude interval from values specified at P node points in the ionosphere, the function of spline surface⁴ can be written as follows

$$\Delta I(\Phi, \Lambda) = \sum_{i=1}^P c_i r_i^2 \ln r_i^2 + c_{P+1} + c_{P+2} \Phi + c_{P+3} \Lambda, \quad (3)$$

where $r_i^2 = (\Phi - \Phi_i)^2 + (\Lambda - \Lambda_i)^2$ is the distance from arbitrary point to the i th node, and c_i are spline coefficients. The coefficients $c_i, j = 1, \dots, (P + 3)$, whose values determine the spline surface $\Delta I(\Phi, \Lambda)$, are found via solution of the system of linear equations:

$$\left. \begin{aligned} \Delta I(\Phi_j, \Lambda_j) &= \sum_{i=1}^P c_i r_{ij}^2 \ln r_{ij}^2 + c_{P+1} + \\ &+ c_{P+2} \Phi_j + c_{P+3} \Lambda_j = \Delta I_j^v, \quad j = 1, \dots, P; \\ \sum_{i=1}^P c_i &= 0; \quad \sum_{i=1}^P \Phi_i c_i = 0; \quad \sum_{i=1}^P \Lambda_i c_i = 0; \\ r_{ij}^2 &= (\Phi_j - \Phi_i)^2 + (\Lambda_j - \Lambda_i)^2. \end{aligned} \right\} \quad (4)$$

Solution of this system exists if $P > 3$, and it is unique if among the points $(\Phi_j, \Lambda_j), j = 1, \dots, P$, there are at least three points not lying on one straight line.⁴

Results and discussion

To assess the quality of reconstruction of the spatial structure of ionospheric perturbation with the use of the method developed, we have compared distribution patterns of TEC increments, obtained after interpolation of values at the ionospheric points, with reference patterns for the corresponding moments in time.

The reference patterns were created by modeling TEC values along vertical paths located at nodes (dots in Fig. 3a) of uniform grid (grid spacing is 0.5°).

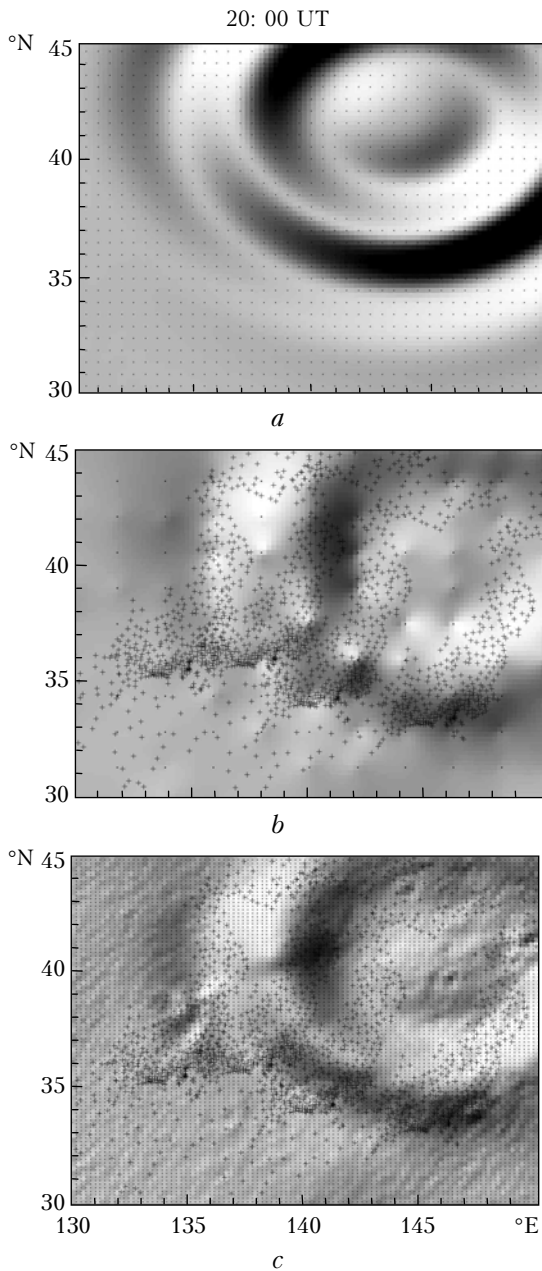


Fig. 3. Reference TEC perturbation structure (*a*) and structure reconstructed using spline interpolation (*b–c*).

Model parameter values were chosen the same as in modeling of TEC measurements. Reference pattern of the spatial structure of ionospheric perturbation at the time $t = 20:00$ UT is presented in Fig. 3*a*. It is seen that the perturbation has the features of circular waves diverging from a pronounced center whose position coincides with the epicenter of the earthquake. The amplitude of perturbation is 0.2 TECU, and its radius is about 550 km.

The spatial structure of the field obtained using spline interpolation of the initial TEC increments at ionospheric points is shown in Figs. 3*b* and *c* (positions of ionospheric points are indicated by crosses). The spline surface $\Delta I(\Phi, \Lambda)$ makes it possible to calculate

TEC increments at any point of the given region. To obtain an image, we have calculated TEC variations at nodes (dots in Figs. 3*b* and *c*) of a uniform grid, common for all moments in time in the interval 19:00–21:18 UT. Figure 3*b* shows function reconstructed on a grid containing 10 points in longitude and 10 points in latitude (10×10), while Fig. 3*c* correspondingly shows reconstruction on the grid 100×100.

Comparison of TEC variations, presented in Figs. 3*b* and *c*, with the reference pattern for this same time shows that in both cases the reconstruction of the spatial structure of perturbation is adequate. The reconstructed perturbation exhibits the features of diverging concentric circular waves. The amplitude and radius of reconstructed perturbation coincide with the corresponding values on the reference pattern.

The quality of reconstruction of the spatial structure of ionospheric perturbation depends on the grid configuration. For a denser grid, there is correspondingly larger methodical error appearing in the form of small-scale noise structure. Nonetheless, the reconstruction of perturbation itself is made more correctly in this case, as is seen from the well pronounced ridge of the main maximum of perturbation and well discernible maximum at its center.

Figures 4*e–h* illustrate the time dynamics of ionospheric perturbation for times 19:51, 19:54, 20:00, and 20:06 UT (100×100 grid). It is seen that, as the time progresses, the first, second, and third maxima of perturbation wave gradually form, and the amplitude of wave, as well as radius of its removal from the center, increases. The obtained dynamics well corresponds to the reference pattern (Figs. 4*a–d*).

Analysis of Fig. 4 shows that the developed method can be used as an additional method of determination of parameters of spread of ionospheric perturbation, for which it is sufficient to analyze the cross-correlation function between two patterns of the spatial distribution of TEC increments for different moments in time.

Conclusion

We have presented the method of reconstruction of spatial structure of ionospheric perturbation, based on the spatial spline interpolation of individual readouts of TEC increments, obtained from data measured at a dense network of GPS receivers. In reconstructing, TEC variations are recalculated to “vertical” value and are subjected to filtering. The set of readouts chosen from all series at a certain moment in time are approximated by a spline surface.

This method was tested in reconstruction of the spatial structure of perturbation simulated for conditions of powerful earthquake near Hokkaido Island on September 25, 2003. It is noteworthy, that the structure of ionospheric perturbation, reconstructed with help of spline interpolation was compared with the reference pattern of TEC variations.

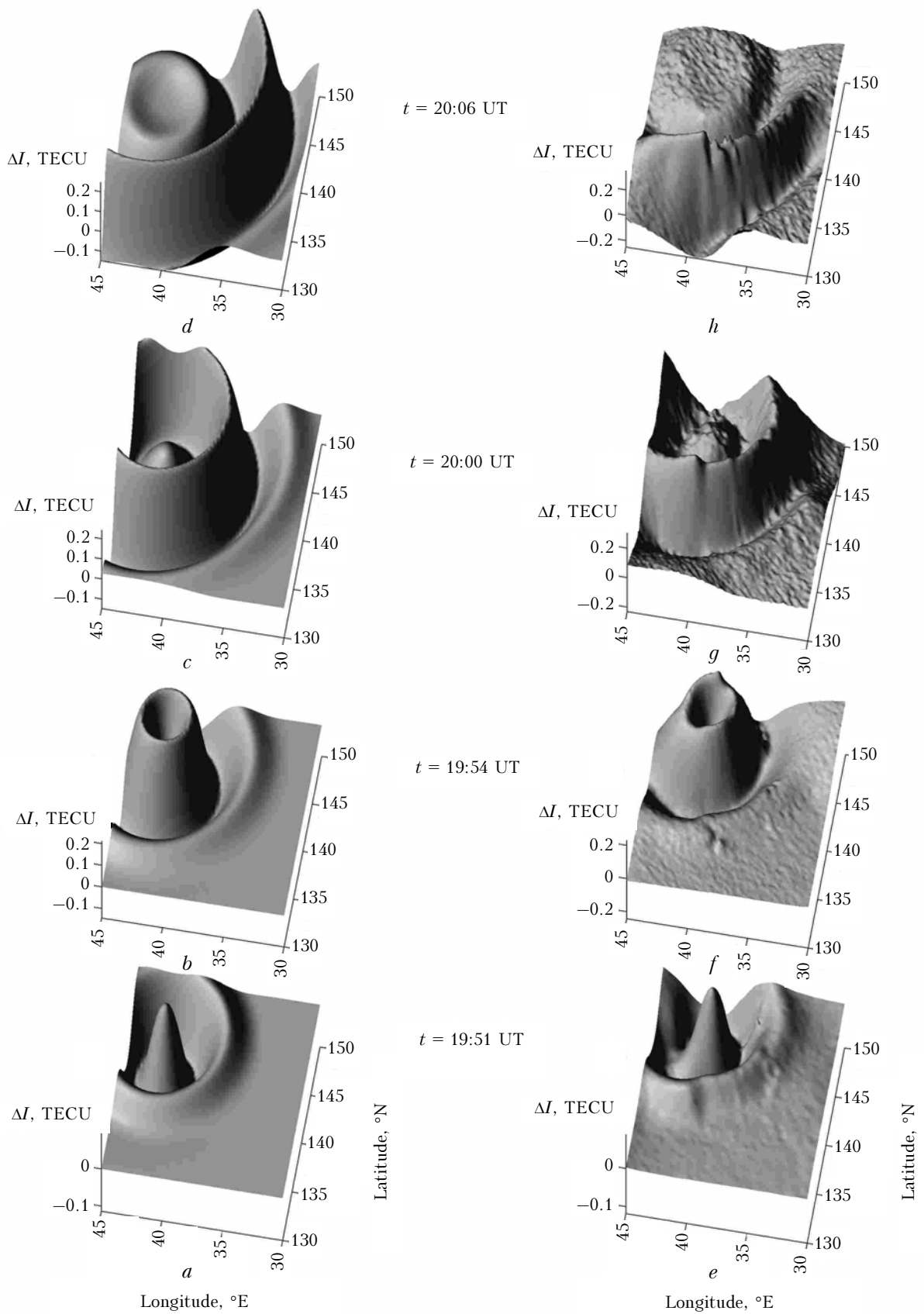


Fig. 4. Time dynamics of ionospheric perturbation: reference pattern (*a–d*) and structure reconstructed using spline interpolation (*e–h*).

The tests have shown that this method is capable of reconstructing the spatial structure of ionospheric perturbation and track the dynamics of its variation with high time resolution.

Acknowledgments

Authors thank Prof. K. Heki from Hokkaido University for providing coordinates of receiving stations of GEONET network.

This work was supported by Russian Foundation for Basic Research (grants Nos. 05–05–64634 and 06–05–64577), as well as by Integration Project of SB RAS No. 3.24.

References

1. A.J. Mannucci, C.M. Ho, and U.J. Lindqwister, *Radio Sci.* **33**, No. 8, 565–582 (1998).
2. A. Saito, S. Fukao, and S. Miyazaki, *Geophys. Res. Lett.* **25**, No. 16, 3079–3082 (1998).
3. S.A. Smolyak, *Ekonomika i Matematicheskie Metody* **7**, Issue 3, 419–431 (1971).
4. R.L. Harder and R.N. Desmarais, *J. of Aircraft.* **9**, No. 2, 189–191 (1972).
5. E.L. Afraimovich, N.P. Perevalova, A.V. Plotnikov, and A.M. Uralov, *Ann. Geophys.* **19**, No. 4, 395–409 (2001).
6. G.V. Rudenko and A.M. Uralov, *J. Atmos. and Terr. Phys.* **57**, No. 3, 225–236 (1995).
7. E.L. Afraimovich, E.I. Astaf'eva, and V.V. Kiryushkin, *Radiophys. and Quantum. Electron.* **48**, No. 4, 299–313 (2005).